

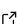

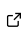
# 1 AQCNES: A Quasi-Continuum Non-Equilibrium Solver

2 **Gerhard Bräunlich** <sup>3\*</sup>, **Shashank Saxena** <sup>1\*</sup>, **Manuel Weberndorfer**<sup>3</sup>,  
3 **Miguel Spinola** <sup>1</sup>, **Prateek Gupta** <sup>2\*</sup>, and **Dennis M. Kochmann** <sup>1</sup>

4 **1** Mechanics & Materials Laboratory, ETH Zürich, Switzerland **2** Department of Applied Mechanics,  
5 Indian Institute of Technology Delhi, India **3** Scientific IT Services, ETH Zürich, Switzerland \* These  
6 authors contributed equally.

DOI: [10.xxxxxx/draft](https://doi.org/10.xxxxxx/draft)

## Software

- [Review](#) 
- [Repository](#) 
- [Archive](#) 

Editor: [Philip Cardiff](#) 

## Reviewers:

- [@streeve](#)
- [@T-Hageman](#)

Submitted: 07 May 2024

Published: unpublished

## License

Authors of papers retain copyright  
and release the work under a

Creative Commons Attribution 4.0  
International License ([CC BY 4.0](https://creativecommons.org/licenses/by/4.0/))

## 7 Summary

8 The behavior of macroscopic structures is determined by fast atomic interactions at the  
9 nanoscales. Current atomic simulation techniques, such as molecular dynamics (MD), are  
10 limited to a millions of atoms and hence a few micrometers of domain length. Moreover, finite-  
11 temperature vibrational frequencies of around tens of terahertz restrict the time step of MD to  
12 femtoseconds, precluding the simulation of problems of engineering interest. Consequently,  
13 there has been a significant focus in recent decades on developing multiscale modeling  
14 techniques to extend atomistic accuracy to larger length scales and longer time frames. Existing  
15 techniques, such as the quasicontinuum (QC) method, are restricted to spatial upscaling at  
16 zero temperature, while temporal upscaling methods like the maximum entropy (max-ent)  
17 approach are constrained to fully resolved atomistic simulations at finite temperature.

18 The software introduced here, AQCNES, is a C++-based framework that integrates the spatial-  
19 upscaling technique of the quasicontinuum method with the statistical-mechanics-based tem-  
20 poral upscaling technique known as Gaussian phase packets. Message Passing Interface (MPI)  
21 is employed to enable massive parallelism, which enhances the scalability of the software. This  
22 enables computationally efficient and robust simulations of large atomistic ensembles at finite  
23 temperature.

## 24 Statement of need

25 Commonly used atomic simulation techniques describe the entire ensemble as a collection of  
26 particles, each having a position and velocity in three-dimensional space. This fully refined  
27 spatial representation in state space restricts the possible dimensions of the ensemble to  
28 microscopic scales. Moreover, case studies of material defects using atomistic simulations are  
29 often limited to Molecular Statics (MS) or use unrealistically high loading rates ([Homer et al.,](#)  
30 [2022](#); [Shenoy, 2005](#)). This is unavoidable because finite-temperature MD simulations need  
31 long equilibration times and expensive post-processing techniques ([Frenkel & Ladd, 1984](#)) to  
32 extract relevant thermodynamic information. However, physically relevant material behavior  
33 is observed at finite temperature. Therefore, research in the past decades has focused on  
34 multiscale modeling techniques to advance atomistic simulations to larger length scales and  
35 longer time scales ([Miller & Tadmor, 2009](#); [Wernik & Meguid, 2009](#)).

36 Most research groups working in the broad field of upscaling atomistic simulations have their  
37 proprietary codes. Two available open-source codes are QuasiContinuum ([Miller & Tadmor,](#)  
38 [2012](#)) based on the quasicontinuum (QC) method and MultiBench ([Miller & Tadmor, 2009](#)),  
39 which is an implementation of fourteen popular spatial upscaling methods. However, both  
40 are limited to zero-temperature simulations for crystalline solids in two dimensions. The MXE  
41 package in LAMMPS ([Mendez & Ponga, 2021](#)) is an implementation of the temporal upscaling  
42 technique max-ent for a fully resolved atomic ensemble with no spatial coarse-graining. To

43 the best of the authors' knowledge, there is no such open-source atomistic simulation software  
44 that combines the aforementioned spatial and temporal upscaling techniques.

45 AQCNESS is a software that can predict long-term behavior of large atomic ensembles using  
46 the spatio-temporal upscaling of classical atomistic calculations. It enables the calculation of  
47 material properties at finite (non-zero) temperature from atomic scales, offering promising  
48 applications in solid-state material science across scales. In the present implementation, full  
49 atomistic resolution is needed for regions of local disorder as well as for amorphous materials,  
50 although extension of the QC for amorphous systems have been proposed (Ghareeb & Elbanna,  
51 2020) and can be considered as a possible extension. Hence, AQCNESS is capable of simulating  
52 both crystalline and amorphous materials in a temporally upscaled fashion at zero and non-zero  
53 temperature, while the spatial upscaling capability is limited to crystalline systems. It can  
54 also simulate large atomic rearrangements induced by severe deformations in multi-resolution  
55 domains by using an updated Lagrangian formulation (Gupta et al., 2021). This formulation  
56 uses the relaxed state after every load step as the new reference configuration. An adaptive  
57 neighborhood calculation strategy (similar to Tembhekar et al. (2017)) is adopted, where  
58 the neighborhoods are regenerated if the maximum relative displacement of a neighbor with  
59 respect to a sampling atom exceeds a given buffer radius. This unique combination of features  
60 positions AQCNESS as a versatile and powerful tool in the realm of atomistic simulations.

## 61 Functionality

62 A technique known as Gaussian Phase Packets (GPP) (Gupta et al., 2021) is used to upscale  
63 in time. Instead of the instantaneous phase-space coordinates (position  $\mathbf{q}$  and momentum  
64  $\mathbf{p}$ ), statistical averages  $\{\bar{\mathbf{p}}, \bar{\mathbf{q}}\}$  and variances  $\{\Sigma^{(\mathbf{p},\mathbf{p})}, \Sigma^{(\mathbf{p},\mathbf{q})}, \Sigma^{(\mathbf{q},\mathbf{q})}\}$  of these coordinates are  
65 tracked for the entire ensemble in GPP, thus separating the slow mean atomic motion from fast  
66 atomic vibrations. The covariance matrices represented above are fully populated for the most  
67 general case. However, in order to make the system of equations more tractable, interatomic  
68 correlations are assumed to be zero. Further, intra-atomic covariance matrices are assumed to  
69 be spherical Gaussian clouds. This leads to

$$\Sigma_i^{(\mathbf{p}_i, \mathbf{p}_i)} = \Omega_i \mathbf{I}, \quad \Sigma_i^{(\mathbf{p}_i, \mathbf{q}_i)} = \beta_i \mathbf{I}, \quad \Sigma_i^{(\mathbf{q}_i, \mathbf{q}_i)} = \Sigma_i \mathbf{I}, \quad (1)$$

70 where subscript  $i$  runs over all atoms in the ensemble and  $\mathbf{I}$  is an identity matrix in 3D space.  
71 Hence, the set of variables  $\{\bar{\mathbf{p}}_i, \bar{\mathbf{q}}_i, \Omega_i, \beta_i, \Sigma_i\}$  is solved for every atomic site. It can be shown  
72 that in the quasistatic limit, mean momenta  $\bar{\mathbf{p}}_i$  and thermal momenta  $\beta_i$  vanish for every  
73 atom. The mean positions  $\{\bar{\mathbf{q}}_i : i = 1, \dots, N\}$  and position variances  $\{\Sigma_i : i = 1, \dots, N\}$  are  
74 obtained using the following equilibrium conditions (Gupta et al., 2021):

$$\langle \mathbf{F}_i \rangle = \mathbf{0} \quad \text{and} \quad \frac{\Omega_i}{m_i} + \frac{\langle \mathbf{F}_i(\mathbf{q}) \cdot (\mathbf{q} - \bar{\mathbf{q}}) \rangle}{3} = 0, \quad (2)$$

75 where  $\mathbf{F}_i$  denotes the net force acting on atom  $i$  having mass  $m_i$ . Information about momentum  
76 variances  $\{\Omega_i : i = 1, \dots, N\}$  is obtained from the thermodynamic process which brings  
77 the system to equilibrium. The governing equations (2) of these statistical parameters can  
78 be shown to yield configurations which minimize a thermalized Helmholtz free-energy at the  
79 temperature of interest. The reader is referred to Gupta et al. (2021) for further details.  
80 AQCNESS uses FIRE (Bitzek et al., 2006) to relax the system of equations (2) and thus obtain a  
81 thermodynamically relaxed structure of the ensemble after a quasi-static minimization. This  
82 approach is more robust and computationally efficient (Saxena et al., 2022) than tracking  
83 individual atomic trajectories. Moreover, it makes the simulation of realistic and quasistatic  
84 loading scenarios possible, in contrast to the unrealistically high strain rates accessible by MD  
85 simulations (Vu-Bac et al., 2014; Zhao et al., 2010).

	No. of atoms	No. of procs.	No. of iterations	Simulation time (min)
AQCNES	2624	25	767	9.79
LAMMPS	16400	128	$4.8 \cdot 10^7$	422

**Table 1:** Simulation times for a surface free energy computation for the (001) surface in Fe at 300 K with AQCNES and thermodynamic integration in LAMMPS (adapted from Saxena et al. (2022)).

86 For spatial coarse-graining, AQCNES uses QC (Miller & Tadmor, 2002; Tadmor, 1996). QC  
 87 exploits the long-range order in crystalline materials to explicitly model  $N^h \ll N$  repre-  
 88 sentative(*rep*-) atoms in the domain and uses techniques from continuum-level finite-element  
 89 modeling to obtain all other atomic degrees of freedom as a function of those of the repre-  
 90 sentative atoms. Fully atomistic resolution is retained in the vicinity of material defects, where  
 91 the long-range order is broken. The mean position  $\bar{\mathbf{q}}_i$  and position variance  $\Sigma_i$  of an atom  $i$   
 92 are obtained by the following interpolation:

$$\bar{\mathbf{q}}_i = \sum_{a=1}^{N^h} N_a(\bar{\mathbf{X}}_i) \bar{\mathbf{q}}_a, \quad \Sigma_i = \sum_{a=1}^{N^h} N_a(\bar{\mathbf{X}}_i) \Sigma_a, \quad (3)$$

93 where  $N_a(\bar{\mathbf{X}}_i)$  is the shape function for repatom  $a$  evaluated at the position of atom  $i$  in the  
 94 reference configuration. This reduces the number of degrees of freedom to solve from  $4N$  to  
 95  $4N^h$  for finite-temperature simulations. For energy and force calculation in every minimisation  
 96 iteration, a set of  $N^s \ll N$  sampling atoms is selected. The approximate Hamiltonian of the  
 97 entire system can then be written as:

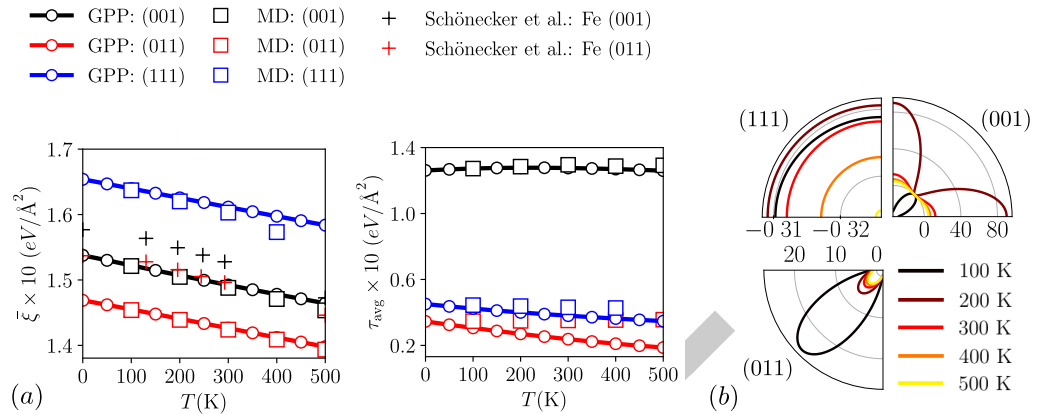
$$\mathcal{H} \approx \sum_{\alpha=1}^{N^s} w_{\alpha} \mathcal{H}_{\alpha}, \quad (4)$$

98 where  $w_{\alpha}$  are the sampling atom weights and  $\mathcal{H}_{\alpha}$  is the energy of the  $\alpha$ th sampling atom. A  
 99 detailed explanation of optimally choosing sampling atom locations and weights can be found  
 100 in Amelang et al. (2015).

## 101 Example applications

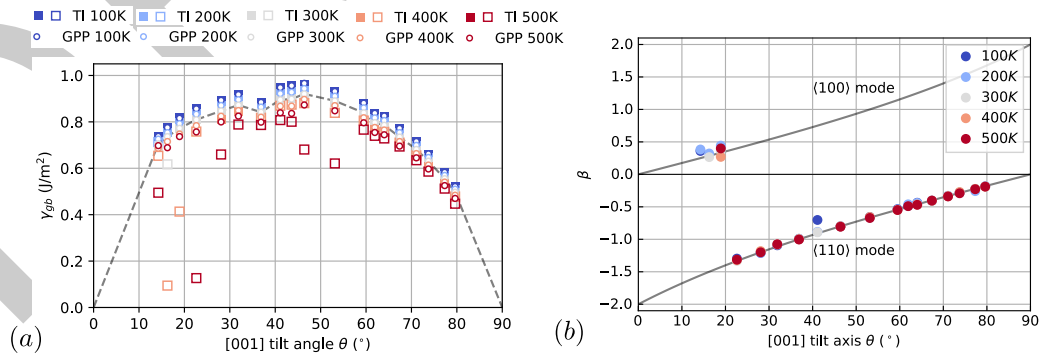
102 The following gives a summary of the mechanics and material science applications where  
 103 AQCNES has already been used:

- 104 ▪ **Surface Elasticity:** Surfaces in solids are the simplest extended defects and contribute  
 105 to excess energy, leading to an inherent stress associated with them. Their presence  
 106 also changes the elastic moduli of the solid as compared to those of the bulk solid.  
 107 AQCNES was used by Saxena et al. (2022) to perform a detailed case study of three  
 108 differently crystallographically oriented surfaces for FCC and BCC metals as a function  
 109 of temperature. The results were also compared against those obtained from state-of-  
 110 the-art thermodynamic integration techniques (Freitas et al., 2016), showing convincing  
 111 accuracy. The comparison of computational times taken by MD and AQCNES (see Table 1)  
 112 shows that there is an approximately fifty-fold computational speedup and a significant  
 113 reduction in the computational resources needed for computing the excess surface free  
 114 energy for an ensemble at finite temperature. Figure 1 shows the surface free energy,  
 115 stresses, and elastic constants for the (001), (011), and (111) surfaces in BCC iron  
 116 computed using AQCNES and their comparison with MD simulations and *ab-initio* results  
 117 by Schönecker et al. (2015). The embedded atom method (EAM) potential developed  
 118 by Chamati et al. (2006) was used for AQCNES and MD simulations.



**Figure 1:** (a) Surface free energy density ( $\xi$ ) and average surface stress ( $\tau_{avg}$ ) vs. temperature ( $T$ ) and (b) polar compliance plots (in Å<sup>2</sup>/eV) for the (001), (011), and (111) surfaces in BCC iron (adapted from Saxena et al. (2022)).

119 ■ **Grain Boundaries:** Grain boundaries (GBs) are regions of crystallographic mismatch  
 120 between two differently oriented grains. They significantly influence the mechanical and  
 121 thermal properties of polycrystalline materials. Hence, investigating GB properties via  
 122 atomic simulations is of scientific interest in the material science community. AQCNESS  
 123 has been used to find relaxed energies of [001] and [011] symmetric-tilt GBs in copper  
 124 as a function of temperature for a range of tilt angles (Spínola et al., 2024). Different  
 125 metastable states have been explored for each temperature and tilt angle. In addition,  
 126 the lowest-energy metastable state was subjected to a quasistatic displacement-driven  
 127 shear to obtain the shear coupling factor of all grain boundaries. AQCNESS could also  
 128 identify the Helmholtz free energy of bicrystals, for which the standard thermodynamic  
 129 integration techniques failed due to hops of the system from one metastable state to  
 130 another. Figure 2 summarizes the excess grain boundary free energy density and the  
 131 shear coupling factors for the lowest energy metastable state of [001] tilt axis grain  
 132 boundaries in copper. The EAM potential developed by Mishin et al. (2001) was used  
 133 for these simulations.



**Figure 2:** (a) Excess grain boundary free energy density ( $\gamma_{gb}$ ) and (b) shear coupling factor ( $\beta$ ) vs. tilt angle for the [001] symmetric tilt grain boundaries in copper at different temperatures (adapted from Spínola et al. (2024)).

134 ■ **Nanoindentation:**  
 135 Nanoindentation is a widely used technique to probe the mechanical properties of  
 136 materials and nanostructures. AQCNESS has been used to simulate the three-dimensional  
 137 thermo-mechanically-coupled nanoindentation of copper (Gupta et al., 2021). Two layers  
 138 of spatial coarse graining were used to simulate a cube of side length 0.077μm with 0.2  
 139 million representative atoms. The complicated microstructure of prismatic dislocation

140 loops below the nanoindenter could be observed in the finite-temperature simulations  
 141 at 300 and 600 K. The temperature dependence of the critical indenter force before  
 142 dislocation nucleation could also be captured. Figure 3 shows the microstructure below  
 143 the indenter and the indenter force for different temperatures.

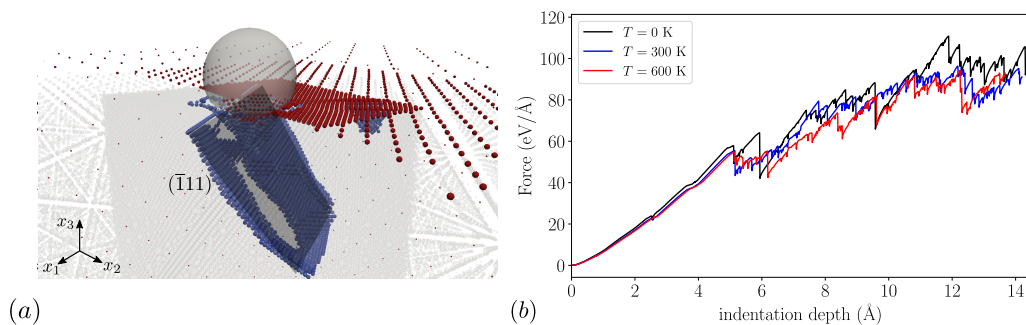


Figure 3: (a) Dislocation loops generated as a result of nanoindentation beneath the spherical indenter at a depth of 1 nm. (b) Indenter force vs. depth for isothermal nanoindentation at different temperatures (adapted from Gupta et al. (2021)).

## 144 Dependencies and API documentation

145 The project uses CMake as its build system generator. The following third party libraries are  
 146 required and located using CMake's find\_package.

- 147 ■ Boost (components: program\_options, mpi, serialization): version 1.67
- 148 ■ Eigen: version 3.4
- 149 ■ MPI: version 3.1
- 150 ■ PETSc: version 3.15
- 151 ■ CGAL: version 5.4
- 152 ■ PnetCDF: Version 1.12
- 153 ■ nlohmannjson: Version 3.10
- 154 ■ Scotch/ParMETIS
- 155 ■ qcmesh: Version 1.0
- 156 ■ VTK: Version 9.3

157 The dependency versions mentioned above are not strictly the minimum versions required, but  
 158 the ones which have been tested to work well. The code quality of the project is analyzed in a  
 159 CI pipeline which runs inside the development docker container and on the ETH HPC cluster  
 160 Euler. The pipeline covers the following checks:

- 161 ■ Building the docker container and publishing it to registry.gitlab.ethz.ch.
- 162 ■ Building documentation and publishing it to qc.mm.ethz.ch.
- 163 ■ Code compilation and running unit/integration tests.
- 164 ■ Presence of a license header for each source file.
- 165 ■ Consistency of code formatting using clang-format for C++ and ruff for Python.
- 166 ■ Static code analysis (linter) using clang-tidy for C++ and ruff for Python.

167 Detailed documentation of the API can be found on the AQCNES website, and simple examples  
 168 to get started can be found here. Importantly, the use of AQCNES is not limited to these  
 169 examples and the ones listed in this contribution.

170 **Acknowledgements**

171 The support from the European Research Council (ERC) under the European Union's Horizon  
172 2020 research and innovation program (grant agreement no. 770754) is gratefully acknowledged.  
173 We also acknowledge contributions to the code from Stefan Zimmerman and Anny Wang.

174 **References**

- 175 Amelang, J. S., Venturini, G. N., & Kochmann, D. M. (2015). Summation rules for a fully  
176 nonlocal energy-based quasicontinuum method. *Journal of the Mechanics and Physics of*  
177 *Solids*, 82, 378–413.
- 178 Bitzek, E., Koskinen, P., Gähler, F., Moseler, M., & Gumbsch, P. (2006). Structural relaxation  
179 made simple. *Physical Review Letters*, 97(17), 170201.
- 180 Chamati, H., Papanicolaou, N., Mishin, Y., & Papaconstantopoulos, D. (2006). Embedded-  
181 atom potential for fe and its application to self-diffusion on fe (1 0 0). *Surface Science*,  
182 600(9), 1793–1803.
- 183 Freitas, R., Asta, M., & De Koning, M. (2016). Nonequilibrium free-energy calculation of  
184 solids using LAMMPS. *Computational Materials Science*, 112, 333–341.
- 185 Frenkel, D., & Ladd, A. J. (1984). New monte carlo method to compute the free energy of  
186 arbitrary solids. Application to the fcc and hcp phases of hard spheres. *The Journal of*  
187 *Chemical Physics*, 81(7), 3188–3193.
- 188 Ghareeb, A., & Elbanna, A. (2020). An adaptive quasicontinuum approach for modeling  
189 fracture in networked materials: Application to modeling of polymer networks. *Journal of*  
190 *the Mechanics and Physics of Solids*, 137, 103819.
- 191 Gupta, P., Ortiz, M., & Kochmann, D. M. (2021). Nonequilibrium thermomechanics of  
192 gaussian phase packet crystals: Application to the quasistatic quasicontinuum method.  
193 *Journal of the Mechanics and Physics of Solids*, 153, 104495.
- 194 Homer, E. R., Hart, G. L., Owens, C. B., Hensley, D. M., Spendlove, J. C., & Serafin, L. H.  
195 (2022). Examination of computed aluminum grain boundary structures and energies that  
196 span the 5D space of crystallographic character. *Acta Materialia*, 234, 118006.
- 197 Mendez, J. P., & Ponga, M. (2021). MXE: A package for simulating long-term diffusive  
198 mass transport phenomena in nanoscale systems. *Computer Physics Communications*, 260,  
199 107315.
- 200 Miller, & Tadmor, E. B. (2002). The quasicontinuum method: Overview, applications and  
201 current directions. *Journal of Computer-Aided Materials Design*, 9(3), 203–239.
- 202 Miller, & Tadmor, E. B. (2009). A unified framework and performance benchmark of fourteen  
203 multiscale atomistic/continuum coupling methods. *Modelling and Simulation in Materials*  
204 *Science and Engineering*, 17(5), 053001.
- 205 Miller, & Tadmor, E. B. (2012). *Quasicontinuum method*. [https://doi.org/doi:10.4231/](https://doi.org/doi:10.4231/D3X05XD4W)  
206 [D3X05XD4W](https://doi.org/doi:10.4231/D3X05XD4W)
- 207 Mishin, Y., Mehl, M., Papaconstantopoulos, D., Voter, A., & Kress, J. (2001). Structural  
208 stability and lattice defects in copper: Ab initio, tight-binding, and embedded-atom  
209 calculations. *Physical Review B*, 63(22), 224106.
- 210 Saxena, S., Spinola, M., Gupta, P., & Kochmann, D. M. (2022). A fast atomistic approach to  
211 finite-temperature surface elasticity of crystalline solids. *Computational Materials Science*,  
212 211, 111511.
- 213 Schönecker, S., Li, X., Johansson, B., Kwon, S. K., & Vitos, L. (2015). Thermal surface free

- 214 energy and stress of iron. *Scientific Reports*, 5(1), 1–7.
- 215 Shenoy, V. B. (2005). Atomistic calculations of elastic properties of metallic fcc crystal surfaces.  
216 *Physical Review B*, 71(9), 094104.
- 217 Spínola, M., Saxena, S., Gupta, P., Runnels, B., & Kochmann, D. M. (2024). Finite-  
218 temperature grain boundary properties from quasistatic atomistics. *arXiv Preprint*  
219 *arXiv:2402.12247*.
- 220 Tadmor, E. B. (1996). *The quasicontinuum method. Modeling microstructure on multiple*  
221 *length scales: A mixed continuum and atomistics approach*. Brown University.
- 222 Tembhekar, I., Amelang, J. S., Munk, L., & Kochmann, D. M. (2017). Automatic adaptivity  
223 in the fully nonlocal quasicontinuum method for coarse-grained atomistic simulations.  
224 *International Journal for Numerical Methods in Engineering*, 110(9), 878–900.
- 225 Vu-Bac, N., Lahmer, T., Keitel, H., Zhao, J., Zhuang, X., & Rabczuk, T. (2014). Stochastic  
226 predictions of bulk properties of amorphous polyethylene based on molecular dynamics  
227 simulations. *Mechanics of Materials*, 68, 70–84.
- 228 Wernik, J., & Meguid, S. A. (2009). Coupling atomistics and continuum in solids: Status,  
229 prospects, and challenges. *International Journal of Mechanics and Materials in Design*, 5,  
230 79–110.
- 231 Zhao, J., Nagao, S., & Zhang, Z. (2010). Thermomechanical properties dependence on chain  
232 length in bulk polyethylene: Coarse-grained molecular dynamics simulations. *Journal of*  
233 *Materials Research*, 25, 537–544.

DRAFT